

# c-fms blockade reverses glomerular macrophage infiltration and halts development of crescentic anti-GBM glomerulonephritis in the rat

Yingjie Han<sup>1</sup>, Frank Y Ma<sup>1</sup>, Greg H Tesch<sup>1</sup>, Carl L Manthey<sup>2</sup> and David J Nikolic-Paterson<sup>1</sup>

Depletion and adoptive transfer studies have demonstrated that macrophages induce glomerular lesions in experimental anti-glomerular basement membrane (anti-GBM) glomerulonephritis. However, there is no current therapeutic strategy that can rapidly and selectively remove these cells from the glomerulus in order to halt disease development. This study examined whether inhibition of the receptor for macrophage colony-stimulating factor (known as c-fms), which is selectively expressed by monocyte/macrophages, can eliminate the macrophage infiltrate in a rat model of crescentic anti-GBM glomerulonephritis. Wistar–Kyoto rats were treated with 10 or 30 mg/kg bid of fms-I (a selective c-fms kinase inhibitor) from the time of anti-GBM serum injection until being killed 1, 5 or 14 days later. fms-I treatment had only a minor effect upon the glomerular macrophage infiltrate on day 1 and did not prevent the subsequent induction of proteinuria. However, fms-I treatment reduced the glomerular macrophage infiltrate by 60% at day 5 and completely reversed the macrophage infiltrate by day 14. In addition, fms-I treatment downregulated the glomerular expression of pro-inflammatory molecules (TNF- $\alpha$ , NOS2, MMP-12, CCL2 and IL-12) on days 1 and 5, suggesting a suppression of the macrophage M1-type response. Despite a significant early loss of glomerular podocytes, ongoing proteinuria and glomerular tuft adhesions to Bowman's capsule, the reversal of the macrophage infiltrate prevented the development of glomerulosclerosis, crescent formation, tubulointerstitial damage and renal dysfunction. In conclusion, this study has identified c-fms kinase inhibition as a selective approach to target infiltrating macrophages in acute glomerular injury, which may have therapeutic potential in rapidly progressive crescentic glomerulonephritis.

*Laboratory Investigation* (2011) 91, 978–991; doi:10.1038/labinvest.2011.61; published online 25 April 2011

**KEYWORDS:** c-fms; crescent; dendritic cell; macrophage; podocyte; proteinuria

Macrophages are considered important effector cells in rapidly progressive glomerulonephritis based on their location in lesions, pro-inflammatory phenotype, tight correlation of the macrophage infiltrate with renal dysfunction and histological damage, and their prognostic significance for disease progression.<sup>1</sup> However, current non-selective immunosuppressive drugs do not effectively target this population of immune cells, and this is a major limitation of current treatment.<sup>2</sup>

Animal studies have shown that macrophage deletion can prevent the development of crescentic glomerulonephritis, and replacement of this macrophage population can recapitulate acute glomerular injury.<sup>3–7</sup> However, few experimental strategies have been shown to rapidly reverse a

pro-inflammatory macrophage infiltrate, and such strategies are not clinically applicable. To address this important issue, we have investigated selective inhibition of c-fms—the receptor for macrophage colony-stimulating factor (M-CSF). While M-CSF (also known as CSF-1) is expressed in many tissues, being upregulated in many types of tissue injury, c-fms expression is restricted to cells of the monocyte/macrophage lineage in the adult.<sup>8</sup> M-CSF has a critical role in monocyte production in the bone marrow, and has an important anti-apoptotic role to maintain macrophage populations.<sup>8</sup> M-CSF production is markedly upregulated in the glomerulus and tubulointerstitium in human and experimental rapidly progressive glomerulonephritis.<sup>9,10</sup> Indeed, there is substantial local proliferation of infiltrating monocyte/macrophages in

<sup>1</sup>Department of Nephrology and Monash University Department of Medicine, Monash Medical Centre, Clayton, VIC, Australia and <sup>2</sup>Johnson and Johnson Pharmaceutical Research and Development, L.L.C., Spring House, PA, USA  
Correspondence: Dr DJ Nikolic-Paterson, DPhil, Department of Nephrology, Monash Medical Centre, 246 Clayton Road, Clayton, VIC 3168, Australia.  
E-mail: david.nikolic-paterson@med.monash.edu.au

Part of this work was presented at the Annual Meeting of the American Society of Nephrology, Philadelphia, 2008.

Received 20 October 2010; revised 1 March 2011; accepted 1 March 2011

human and experimental rapidly progressive glomerulonephritis in association with local upregulation of M-CSF expression.<sup>9</sup> Furthermore, elevated circulating levels of M-CSF accelerate crescentic lupus nephritis in MRL-*fas*<sup>lpr</sup> mice.<sup>11</sup>

These data identify the M-CSF/c-fms interaction as a potential therapeutic target. A recently described inhibitor of the tyrosine kinase activity of the c-fms receptor, called fms-I, has been shown to selectively inhibit interstitial macrophage accumulation in the obstructed kidney.<sup>12</sup> The aim of the current study was to determine whether blockade of c-fms could reverse the glomerular macrophage infiltrate in a model of crescentic glomerulonephritis and thereby halt disease progression.

## MATERIALS AND METHODS

### Antibodies and Reagents

Primary antibodies (mouse anti-rat) were CD68 (ED1),  $\alpha\beta$  T cell receptor (R73), PC-10 (anti-proliferating cell nuclear antigen, PCNA), MHC class II (OX-6) and CD11c (8A2) (Serotec, Oxford, UK); vimentin (Dako, Glostrup, Denmark); osteopontin (MPIO-B10, University of Iowa, IA, USA);  $\alpha$ -SMA (Sigma-Aldrich, Castle Hill, NSW, Australia). Polyclonal antibodies included goat anti-collagen IV and rabbit anti-Wilm's tumor antigen 1 (WT-1) (Santa Cruz Biotechnology, Santa Cruz, CA, USA); biotinylated goat anti-mouse IgG and rabbit anti-goat IgG (Zymed-Invitrogen, Carlsbad, CA, USA), horseradish peroxidase-conjugated goat anti-mouse IgG, peroxidase-conjugated mouse anti-peroxidase complexes, and FITC-conjugated rabbit anti-rat IgG and anti-sheep IgG (Dako).

fms-I (4-cyano-1H-imidazole-2-carboxylic acid {2-cyclohex-1-enyl-4-[1-(2-methanesulfonyl-ethyl)-piperidin-4-yl]-phenyl}-amide) is a selective inhibitor of c-fms tyrosine kinase and was synthesized by Johnson and Johnson Pharmaceutical Research and Development.<sup>12</sup> fms-I shows activity against four receptor kinases in cell-based assays with the following IC<sub>50</sub> values ( $\mu$ M): c-fms, 0.0031; c-kit, 0.21; Flt-3, 0.098; Trk-A, 0.50.<sup>12</sup>

### Rat Model of Anti-GBM Glomerulonephritis

Male Wistar-Kyoto rats (180–200 g) were obtained from the Animal Resource Centre, Perth, Australia. All animal experimentation was approved by the Monash Medical Centre Animal Ethics Committee. Groups of eight rats were immunized with 1 mg of sheep IgG in Freund's complete adjuvant followed 5 days later (day 0) by tail vein injection of sheep anti-rat glomerular basement membrane (GBM) serum. Animals were untreated or given fms-I (10 or 30 mg/kg bid) or vehicle alone (20% hydroxylpropyl- $\beta$ -cyclodextrin in H<sub>2</sub>O) by oral gavage beginning 2 h before anti-GBM serum injection and continued twice daily until rats were killed on day 14. Overnight urine (22 h) was collected on days 1, 5 and 14. In a second study of anti-GBM disease, groups of four rats were treated with fms-I (30 mg/kg bid) or vehicle alone as described above, and then killed on day 1 or 5. In addition,

a separate study was performed in normal Wistar rats (no anti-GBM disease) to assess any possible bioactivity of the vehicle. A group of four normal Wistar rats was gavaged twice daily for 5 days and then killed and compared with normal Wistar rats with no intervention.

Blood was collected at the time of death. Analysis of serum creatinine was performed by the Department of Biochemistry, Monash Medical Centre. White blood cell counts were performed when animals were killed using heparinized blood with a Cell Dyn 3500 Cell Counter (Abbott Laboratories, Abbott Park, IL, USA). Urine protein levels were quantified using a Coomassie (Bradford) Protein Assay Kit (Thermo Fisher Scientific, Rockland, IL, USA).

### Histology

Glomerular pathology was scored on PAS section on day 14 of anti-GBM disease. Each full-sized glomerular cross-section (gcs) within the section (>50) was examined under high power ( $\times$  400) and scored for the presence of one or more of hyalinosis, fibrinoid necrosis, atrophy and sclerosis based on the proportion of the glomerulus involved: 0, normal; 1+, 1–10%; 2+, 10–25%; 3+, 25–50%; 4+, >50% glomerular involvement. The percentage of glomeruli-containing crescents was determined. Glomerular tuft adhesions were defined adhesions as areas (<25% of the circumference of Bowman's capsule) in which there is continuity between the glomerular tuft and Bowman's capsule. Scoring was performed on blinded slides. Phosphotungstic acid-hematoxylin (PTAH) staining was used to visualize fibrin deposition.

### Immunohistochemistry

Immunostaining for MHC class II, CD11c and R73 + T cells was performed on cryostat sections. Staining for ED1,  $\alpha$ -SMA and collagen IV, and double immunostaining for ED1 + PCNA was performed as previously described.<sup>9,12</sup> Periglomerular  $\alpha$ -SMA<sup>+</sup> myofibroblast accumulation in 50 consecutive glomeruli was assessed using 0, no  $\alpha$ -SMA<sup>+</sup> cells; 1+, occasional periglomerular  $\alpha$ -SMA<sup>+</sup> cells; 2+, many but discontinuous  $\alpha$ -SMA<sup>+</sup> cells; 3+, continuous layer of  $\alpha$ -SMA<sup>+</sup> cells surrounding the glomerulus; 4+, multiple layers of  $\alpha$ -SMA<sup>+</sup> cells surrounding the glomerulus.

The number of ED1 + macrophages, ED1 + PCNA + proliferating macrophages, R73 + T cells and WT-1 + podocytes per gcs was counted under high power (>50 gcs per section). Interstitial ED1 + macrophages were quantified by image analysis using fields covering >90% of the cortex using Image-Pro software (Media Cybernetics, Maryland, USA). Interstitial R73 + T cells were counted in >20 high power interstitial fields per section. Vimentin staining of tubular cross-section was assessed in 50 consecutive fields ( $\times$  250) using 0, no positive cells; 1+, few (1 or 2) positive tubular cells in the tubule; 2+, >2, but less than half of cells stained; 3+, more than half of cells stained in the tubule. The percentage of tubular cross-sections exhibiting

osteopontin staining scored in the entire cortex. All scoring was performed on blinded slides.

### Real-Time RT-PCR

RNA extraction using the RiboPure RNA isolation kit (Ambion, Austin, TX, USA) was used for frozen whole kidney samples (day 14), and for glomeruli prepared by differential sieving and then purified under a dissecting microscope (days 1 and 5). Reverse transcription and real-time PCR using Taqman probes together with an 18S internal control was performed as previously described.<sup>13</sup> The primer pairs and probes used were NOS2 (Forward: TTCAGAGTCAAATCCTACCAAG; Reverse: GTGTTGTTGGGCTGGGAATA; Probe: GAAAGAGGAAAAGGACA); CD206 (Forward: GACAGATATGAACAAGCATTCC; Reverse: TGAACATCTGAGAGTCTGTCC; Probe: GTTTGGTTGGATTGAGG); Arginase-1 (Forward: CTCAATGACTGAAGTGGACAA; Reverse: GGTCAGTCCATCAACATCAAA; Probe: GGAAGGAAGAAAGGC); IL-12 (Forward: CTTCTTCATCAGGGACATCATC; Reverse: CCTCTGTCTCCTTCGTCTTTTC; Probe: CCATTCCTACTTCTCC); TNF- $\alpha$  (Forward: CTTATCTACTCCAGGTTCTC T; Reverse: TCTCCTGGTATGAAATGGCAA A; Probe: TCACCCACACCGTCAG); MMP-12 (Forward: GTCACAACAGTGGGAGATAA; Reverse: GGCCACATGGAA GAAATTGAAG; Probe: AGTCCAGCCACCAACA); CD163

(Forward: TGGTTCTTCTTGGAGGTG; Reverse: CTCAGTTCCTTCTCCTTCCTT; Probe: GGTTTCTTTGTTGTGG); CCL2 (Forward: TGACCCATAAATCTGAAGCTAA; Reverse: GGCATCACATTCCAAATCACAC; Probe: ACAACCACCTCAAGCAC).

### Statistics

Data are shown as mean  $\pm$  s.d. and results analyzed using parametric ANOVA with *post hoc* analysis with Bonferroni's post-test for multiple comparisons. Non-parametric data were analyzed by the Kruskal–Wallis ANOVA by ranks using Dunn's post-test for multiple comparisons. All analyses were performed using the software GraphPad Prism 5.0 (GraphPad Software, San Diego, CA, USA).

## RESULTS

### fms-I Reverses Glomerular Macrophage Infiltration

Prominent glomerular and interstitial macrophage accumulation was evident on day 14 of vehicle and untreated anti-GBM disease (Figures 1 and 2). Based upon previous studies,<sup>12</sup> we examined fms-I treatment at a dose which does not affect blood monocyte levels (10 mg/kg), and at a maximum therapeutic dose that significantly reduces blood monocyte levels (30 mg/kg). Treatment with 10 mg/kg fms-I resulted in a 30% and 50% reduction in glomerular and interstitial

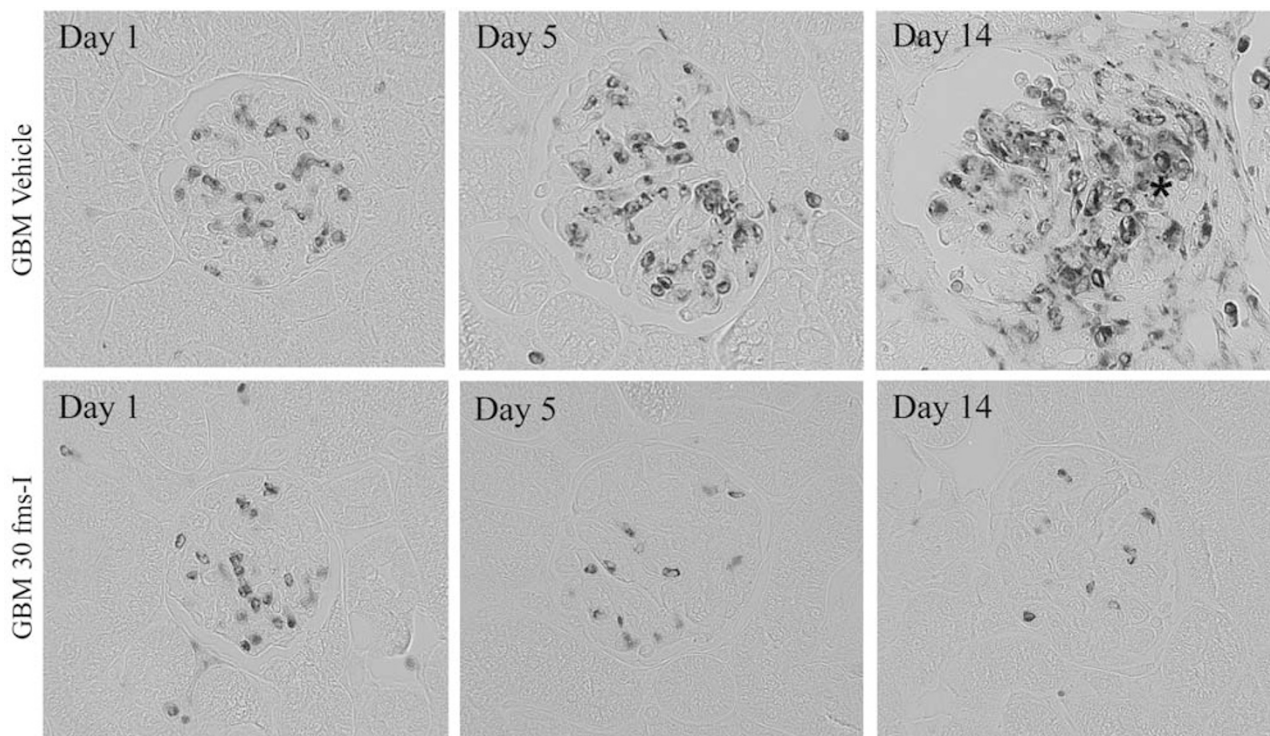


**Figure 1** Immunostaining for glomerular CD68 + macrophages. Top panel shows vehicle-treated anti-GBM disease with a prominent glomerular macrophage infiltrate on day 1, which increases on day 5, with macrophages in the glomerular tuft, in a large cellular crescent (\*), in the periglomerular area and the interstitium on day 14. Lower panel shows high-dose fms-I-treated (30 fms-I) anti-GBM disease in which a prominent macrophage infiltrate was seen on day 1 which was reduced by day 5 and almost entirely eliminated by day 14. Magnification,  $\times 400$ .

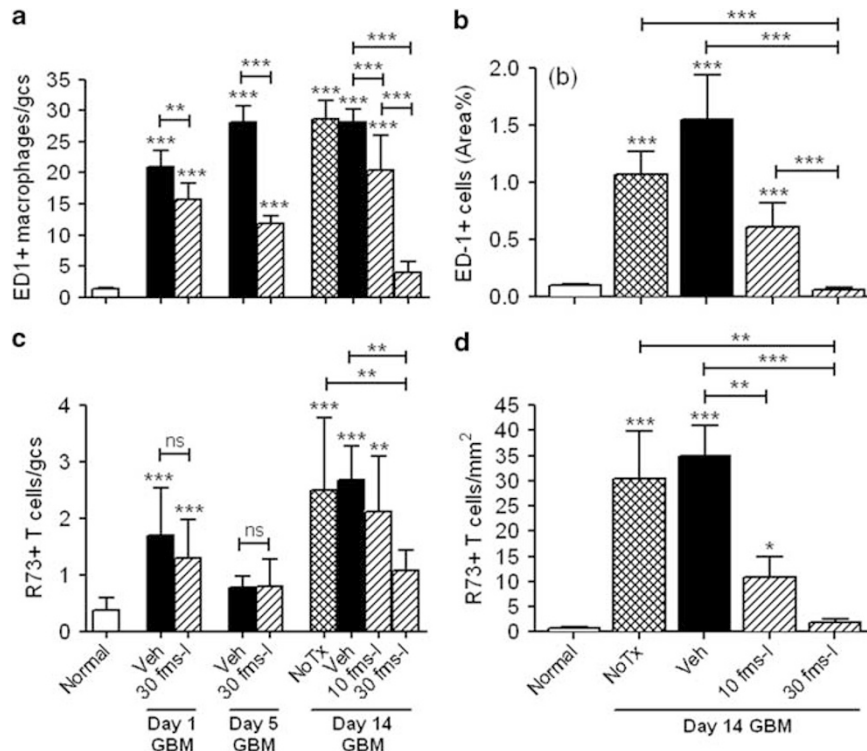


**Figure 2** Quantification of leukocyte accumulation in rat anti-GBM disease. (a) Glomerular CD68 + macrophages on days 1, 5 and 14; (b) area of interstitial CD68 + macrophage staining on day 14. (c) Glomerular T cells on days 1, 5 and 14; (d) interstitial T cells on day 14. A group of normal rats (no anti-GBM disease) is also shown. Data are mean  $\pm$  s.d. \* $P < 0.05$ ; \*\* $P < 0.01$ ; \*\*\* $P < 0.001$  vs normal or for specified comparison by ANOVA with *post hoc* analysis.

macrophages, respectively, on day 14 anti-GBM disease, while treatment with 30 mg/kg fms-I prevented glomerular and interstitial macrophage accumulation (Figures 1 and 2). Figure 3 shows that low-dose fms-I treatment had no effect upon blood leukocyte numbers, while high-dose fms-I markedly suppressed blood monocyte numbers and caused a partial reduction in lymphocyte numbers at day 14. We also confirmed that vehicle treatment in the absence of anti-GBM disease has no effect upon white blood cell counts, renal structure or mRNA levels of pro-inflammatory molecules (Figure 4).

Next, we examined earlier time points to determine whether high-dose fms-I treatment prevented macrophage infiltration, or reversed an early infiltrate, compared with vehicle-treated anti-GBM disease. The prominent glomerular macrophage infiltrate on day 1 of anti-GBM disease was only reduced by 20% with high-dose fms-I (Figures 1 and 2). However, glomerular macrophages were reduced by 60% on day 5 with high-dose fms-I, demonstrating reversal of a substantial early glomerular macrophage infiltrate.

Local proliferation is a prominent feature of anti-GBM disease which is thought to be M-CSF driven and to contribute to glomerular macrophage accumulation.<sup>10,14</sup> Local proliferation of glomerular macrophage was evident at day 14 in vehicle-treated anti-GBM disease ( $7.37 \pm 1.27$  vs  $0.09 \pm 0.11$  ED1 + PCNA + cells per gcs in normal rats;  $P < 0.001$ ), and this was significantly reduced with low-dose

fms-I treatment ( $3.45 \pm 0.93$  ED1 + PCNA + cells per gcs;  $P < 0.001$  vs vehicle treated). The percentage of glomerular macrophage infiltrate undergoing proliferation at day 14 in anti-GBM disease was also reduced by low-dose fms-I treatment ( $32.7 \pm 5.7\%$  in vehicle vs  $21.2 \pm 4.6\%$  in fms-I;  $P < 0.01$ ). To examine the effect of high-dose fms-I treatment we examined day 5 anti-GBM disease when a significant infiltrate was still evident. We found that high-dose fms-I caused a marked reduction in both the number of proliferating macrophages ( $7.65 \pm 0.99$  in vehicle vs  $2.19 \pm 1.42$  ED1 + PCNA + cells per gcs in high-dose fms-I;  $P < 0.001$ ) and the percentage of glomerular macrophages undergoing proliferation ( $47.3 \pm 2.7\%$  in vehicle vs  $23.4 \pm 6.7\%$  in high-dose fms-I;  $P < 0.001$ ) at day 5 of anti-GBM disease. We also examined apoptosis in day 5 anti-GBM disease by TUNEL staining. Only very occasional apoptotic cells were seen in glomeruli in both vehicle and high-dose fms-I-treated groups at this time indicating no significant induction of glomerular macrophage apoptosis (data not shown).

### fms-I Ameliorates Renal Pathology and Renal Dysfunction

Vehicle and untreated anti-GBM disease developed severe glomerular damage, including hyalinosis, fibronoid necrosis, atrophy and sclerosis. Crescent formation was evident in 60% of glomeruli, with most crescents associated with Bowman's capsule rupture (Figures 5 and 6). Fibrin deposition in

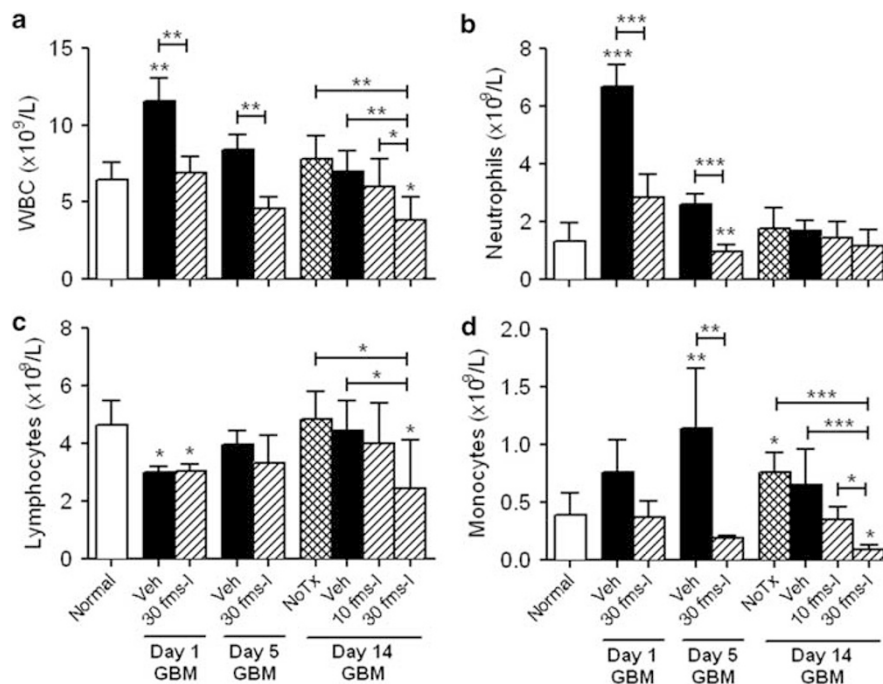


**Figure 3** White blood cell counts on day 14 of anti-GBM disease with no treatment (No Tx), vehicle, low-dose fms-I (10 mg/kg) and high-doses fms-I (30 mg/kg). (a) Total white blood cells; (b) neutrophils; (c) lymphocytes; (d) monocytes. A group of normal rats (no anti-GBM disease) is also shown. Data are mean  $\pm$  s.d. \* $P < 0.05$ ; \*\* $P < 0.01$ ; \*\*\* $P < 0.001$  vs normal or for specified comparison by ANOVA with *post hoc* analysis.

crescents and within Bowman's space was prominent in these rats (Figure 7a). Immunostaining showed deposition of collagen IV in crescents, the glomerular tuft, the periglomerular area and the interstitium which was associated with accumulation of  $\alpha$ -SMA + myofibroblasts (Figure 7). Vehicle and untreated anti-GBM disease also developed marked tubulointerstitial damage with tubular casts, tubular atrophy and interstitial fibrosis (Figures 5 and 7). This severe renal damage was associated with renal dysfunction (Figure 8a).

High-dose fms-I had a profound inhibitory effect on glomerular damage. Crescent formation, Bowman's capsule rupture and fibrin deposition in Bowman's space were prevented, although focal adhesions of the glomerular tuft to Bowman's capsule were still evident in  $34 \pm 10\%$  of glomeruli (Figures 5–7). High-dose fms-I significantly reduced collagen IV deposition in the glomerulus, periglomerular and interstitial areas and abrogated periglomerular and interstitial accumulation of  $\alpha$ -SMA + myofibroblasts (Figures 6d and 7). In addition, high-dose fms-I prevented significant tubulointerstitial injury as seen on PAS-stained sections (Figure 5), and the reduction in tubular expression of vimentin and osteopontin, which are markers of tubular injury (Figure 6e and f). High-dose fms-I also prevented renal dysfunction (Figure 8a).

Despite reducing glomerular macrophage accumulation by only 30%, low-dose fms-I significantly reduced glomerular damage and crescent formation (Figures 5 and 6). In addition, low-dose fms-I significantly reduced periglomerular

$\alpha$ -SMA + myofibroblast accumulation and the development of tubulointerstitial damage in terms of tubular vimentin and osteopontin expression (Figures 5 and 6). Furthermore, low-dose fms-I significantly improved renal function (Figure 8a).

#### fms-I does not Modulate Proteinuria

Vehicle and untreated anti-GBM disease animals developed heavy proteinuria between days 1 and 5 which was associated with a significant reduction in the number of glomerular WT-1 + podocytes (Figure 8b and c). Neither high- nor low-dose fms-I prevented development of proteinuria (Figure 8b). fms-I treatment had a minor protective effect against podocyte loss at day 14 (but not at day 1 or 5), although both fms-I-treated groups still exhibited a substantial reduction in podocyte numbers compared with normal kidney (Figure 8c).

#### fms-I Suppresses Renal Inflammation and Dendritic Cell Infiltration

RT-PCR analysis of isolated glomeruli on days 1 and 5 of vehicle-treated anti-GBM disease identified upregulation of mRNA levels of a number of pro-inflammatory molecules, which are closely associated with the M1-type macrophage response (TNF- $\alpha$ , NOS2, MMP-12, CCL2 and IL-12) (Figure 9a–e). Increased mRNA levels of M2-type markers of alternatively activated macrophages (arginase-1, CD206 and CD163) were also evident (Figure 9f–h). At day 14 of anti-GBM disease, analysis of whole kidney tissue showed ongoing high mRNA levels for the pro-inflammatory molecules

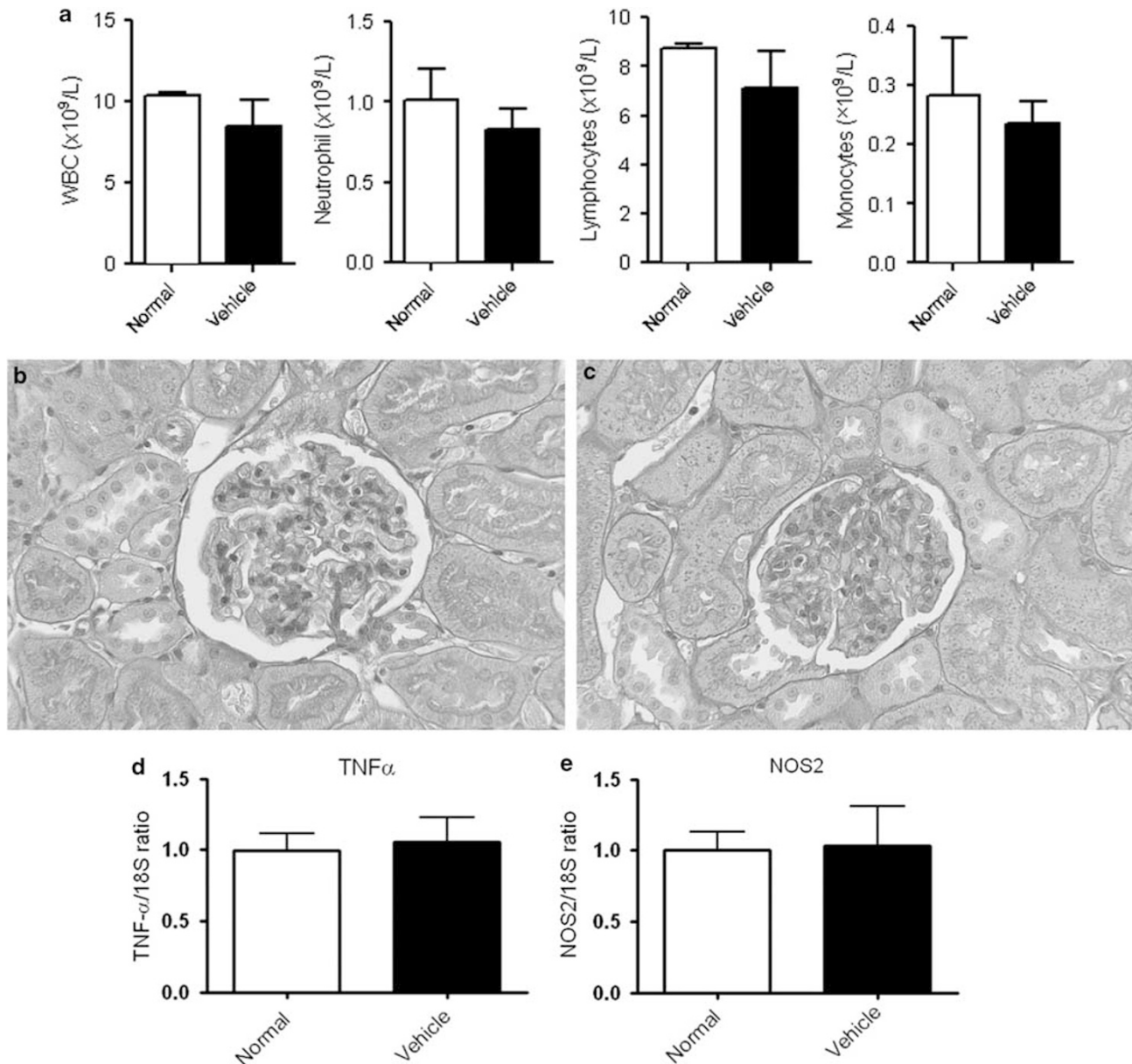


**Figure 4** Analysis of vehicle treatment in normal rats in the absence of anti-GBM disease. A group of four Wistar rats was killed after a 5-day period of twice daily gavage with vehicle (vehicle group), and compared with a group of four untreated rats (normal group). (a) White blood cell counts showing numbers of total white blood cells, neutrophils, lymphocytes and monocytes. PAS staining shows normal kidney structure in a rat with no intervention (b, normal group), and in a vehicle-treated normal rat (c, vehicle group). Analysis of mRNA levels in isolated glomeruli by real-time RT-PCR for (d) TNF- $\alpha$  and (e) NOS2. No differences were seen between the two groups in any of the parameters. Magnification,  $\times 400$  (b, c).

TNF- $\alpha$ , NOS2, MMP-12 and CCL2 (Figure 9i–l). High-dose fms-I abrogated glomerular and interstitial macrophages at day 14 and this prevented the upregulation of mRNA levels for these pro-inflammatory molecules (Figure 9i–l). At earlier time points (days 1 and 5) high-dose fms-I significantly reduced upregulation of mRNA levels for all of the M1-type markers (TNF- $\alpha$ , NOS2, MMP-12, CCL2 and IL-12), while there was a relative increase in expression of the M2-type markers arginase-1 and CD206 (but not CD163) when

considering the reduction in total macrophage numbers with this treatment (Figure 9a–h). Low-dose fms-I had no significant effect upon upregulation of mRNA levels of pro-inflammatory molecule at day 14 (Figure 9i–l).

Untreated and vehicle-treated anti-GBM disease featured an acute glomerular T-cell infiltrate on day 1 which was again evident on day 14—at which time an interstitial T-cell infiltrate was also evident (Figure 2). High-dose fms-I did not affect the early glomerular T-cell infiltrate, but glomerular

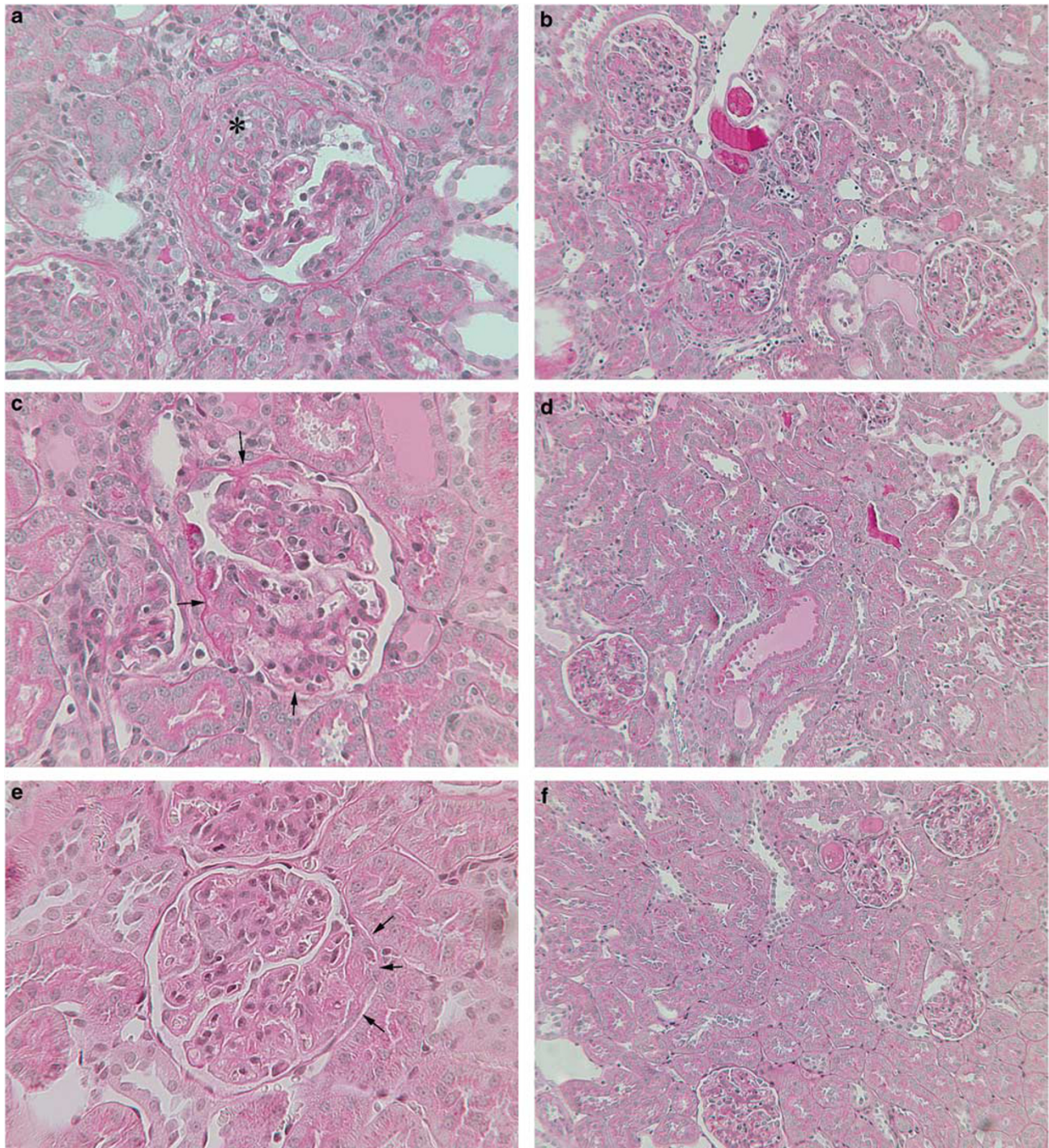


**Figure 5** PAS staining of renal pathology on day 14 of anti-GBM disease. (a) No treatment (No Tx) showing severe glomerular damage with fibrocellular crescent formation (\*) with Bowman's capsule rupture and periglomerular mononuclear cell infiltration, while lower power (b) shows extensive tubular damage, interstitial mononuclear cell infiltration and cast formation. (c) Low-dose fms-I (10 mg/kg) treatment shows moderate glomerular damage with tuft adhesion to Bowman's capsule (arrows), with lower power (d) showing some tubular damage and cast formation. (e) High-dose fms-I (30 mg/kg) shows mild glomerular damage with focal adhesion to Bowman's capsule (arrows), with low power (f) showing little tubulointerstitial damage, although some cast formation is evident. Magnifications,  $\times 400$  (a-c) and  $\times 160$  (d-f).

T cells were reduced on day 14 and the interstitial T-cell infiltrate was prevented (Figure 2). Low-dose fms-I did not affect glomerular T cells on day 14, but it partially reduced

the interstitial T-cell infiltrate (Figure 2). Immunofluorescence staining found no difference between any of the disease groups in the intensity of sheep IgG deposition along

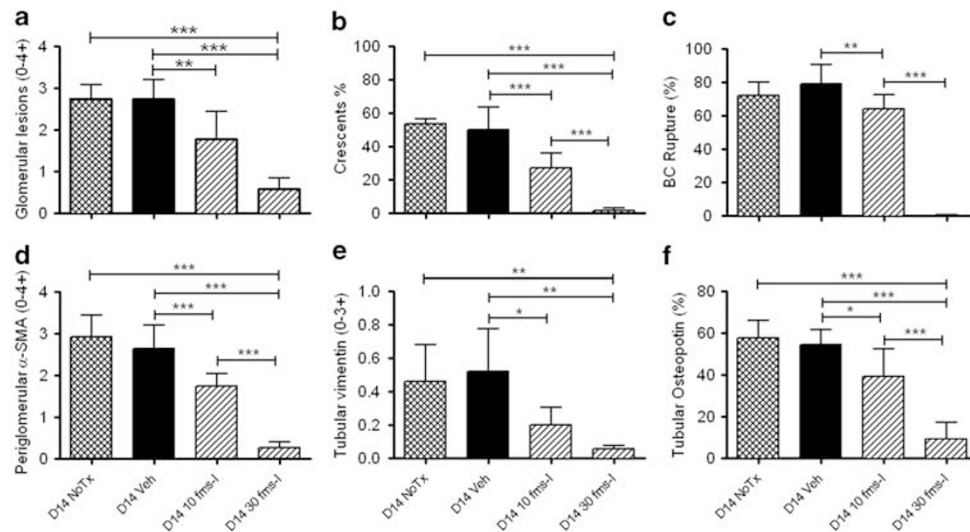


**Figure 6** Quantification of glomerular and tubulointerstitial damage on day 14 of rat anti-GBM disease. (a) Lesions of the glomerular tuft; (b) crescent formation; (c) Bowman's capsule rupture; (d) periglomerular myofibroblast accumulation; (e) tubular vimentin expression; (f) tubular osteopontin expression. Data are mean  $\pm$  s.d. \* $P$ <0.05; \*\* $P$ <0.01; \*\*\* $P$ <0.001 by ANOVA with *post hoc* analysis.

the GBM (data not shown). Similarly, no group differences were found in the intensity of glomerular deposition of rat IgG or C3 (data not shown).

Recent studies have implicated dendritic cells in promoting renal injury.<sup>15</sup> We examined dendritic cells in anti-GBM disease using CD11c and major MHC class II as markers. Normal rat kidney has dendritic-like MHC class II+ cells around Bowman's capsule and within the interstitium, with occasional positive cells in the glomerular tuft (Figure 10). On day 1 of anti-GBM disease, a small glomerular infiltrate of MHC class II+ cells was apparent, and by day 14 many MHC class II+ cells were seen in glomeruli and crescents, and an increase in MHC class II+ cells was observed in the interstitium (Figure 10). CD11c is also expressed by a population of dendritic-like cells in normal rat kidney with a similar distribution to MHC class II+ cells, although fewer in number (Figure 10). A substantial glomerular infiltrate of CD11c+ cells was seen on day 1 of anti-GBM disease, with many CD11c+ cells seen in the glomerulus and interstitium on day 14 (Figure 10).

High-dose fms-I did not affect the glomerular infiltrate of MHC class II+ or CD11c+ cells on day 1 (Figure 10). However, there was a dramatic reduction in glomerular, periglomerular and interstitial MHC class II+ and CD11c+ cells by day 14 (Figure 10).

## DISCUSSION

This study has demonstrated that treatment with fms-I, a c-fms kinase inhibitor, can reverse glomerular macrophage infiltration and prevent the development of crescentic glomerulonephritis despite ongoing proteinuria.

High-dose fms-I had little impact upon the early monocyte recruitment into the glomerulus on day 1 of anti-GBM

disease, but this treatment substantially reduced glomerular macrophages by day 5 and reversed this infiltrate by day 14. Since blood monocyte numbers were not affected by high-dose fms-I in the first 24 h, we can conclude that M-CSF/c-fms signaling is not involved in the initial recruitment of monocytes into the glomerulus following the deposition of anti-GBM antibodies despite M-CSF being a recognized monocyte chemotactic factor.<sup>16</sup> In addition, we can conclude that a sustained glomerular macrophage infiltrate requires M-CSF/c-fms signaling, which is likely to operate via at least two distinct mechanisms. First, M-CSF/c-fms signaling is required for blood monocyte production, and this was suppressed by high-dose fms-I after day 1 thereby preventing further glomerular monocyte recruitment. Second, glomerular macrophage turnover is very rapid in this model based on previous studies showing high levels of local macrophage proliferation within the kidney,<sup>14</sup> and the finding that adoptive transfer studies produce transient glomerular macrophage populations lasting only a few days in this model.<sup>4,17</sup> High-dose fms-I treatment was shown to substantially suppress macrophage proliferation within the glomerulus. However, there was no detectable induction of glomerular cell apoptosis at day 5, the time at which macrophage numbers and proliferation were reduced by high-dose fms-I treatment, suggesting that the macrophages were not dying *in situ* within the kidney. Therefore, the ability of low-dose fms-I to partially reduce the macrophage infiltrate in anti-GBM disease is largely due to inhibition of local macrophage proliferation within the kidney, while the more potent reversal of the glomerular macrophage infiltrate by high-dose fms-I is due to a combination of suppressing blood monocyte counts and inhibition of macrophage proliferation within the kidney.

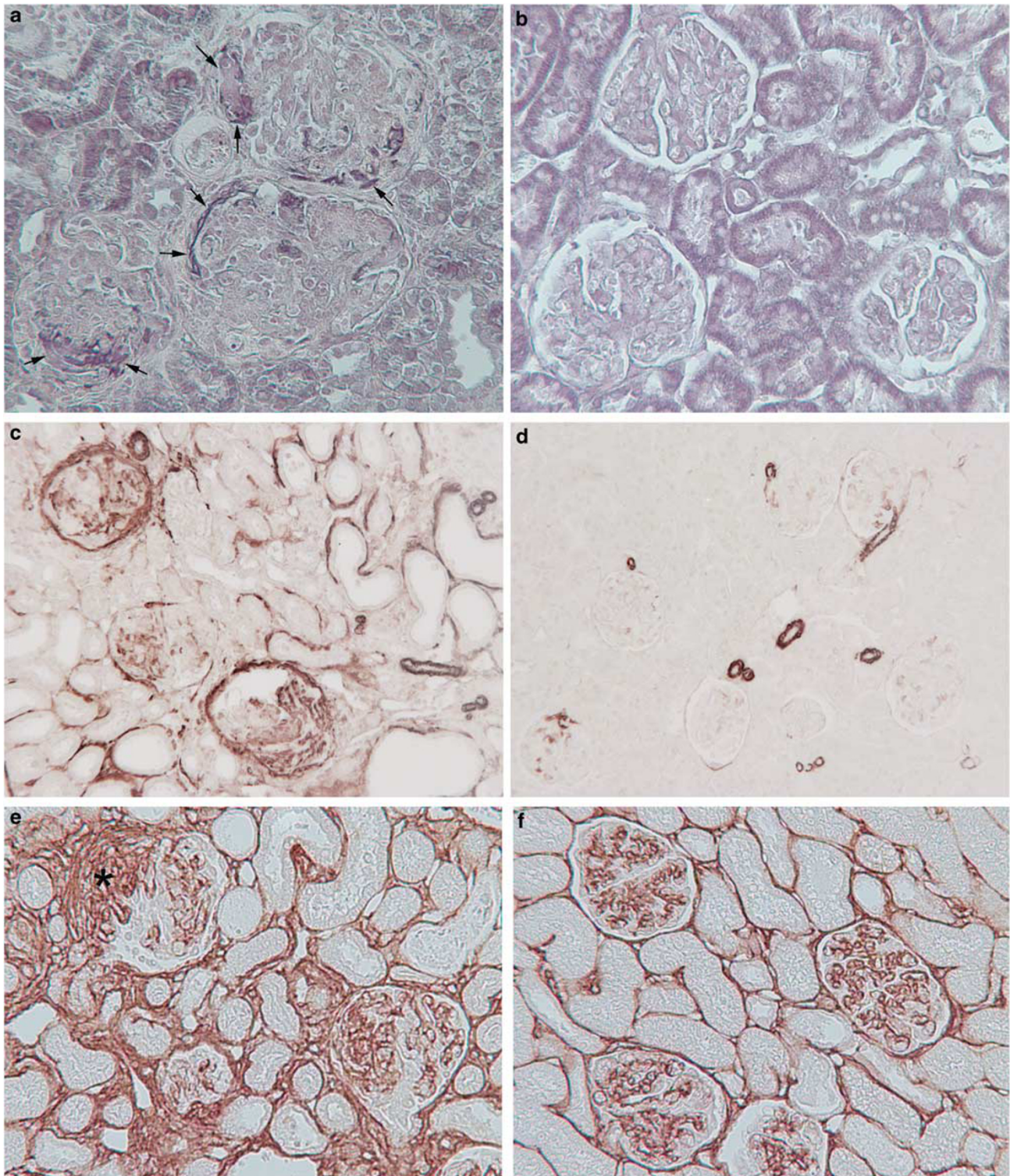


**Figure 7** Histological analysis of day 14 anti-GBM disease. **(a)** PTAH staining shows fibrin deposition (intense blue stain, arrows) in glomerular crescents in vehicle-treated rats, which is; **(b)** absent in rats given high-dose fms-I treatment. **(c)**  $\alpha$ -SMA immunostaining shows myofibroblasts in the glomerular tuft, crescents, the periglomerular area and in an area of damaged tubulointerstitium in vehicle-treated disease, while **(d)** high-dose fms-I treatment largely prevented myofibroblast accumulation. **(e)** Immunostaining shows collagen IV deposition within a crescent (\*), around Bowman's capsule and in the interstitium, which is **(f)** prevented by high-dose fms-I. Magnifications,  $\times 400$  (**a**, **b**);  $\times 160$  (**c**, **d**);  $\times 250$  (**e**, **f**).

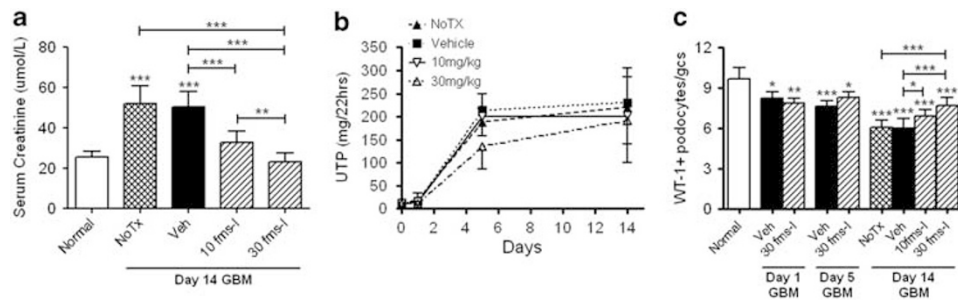


**Figure 8** Renal function and proteinuria in rat anti-GBM disease. **(a)** Graph of serum creatinine on day 14 of disease. **(b)** Graph of proteinuria. **(c)** Graph showing the number of glomerular WT-1 + podocytes. A group of normal rats (no disease) is also shown. Data are mean  $\pm$  s.d. \* $P$ <0.05; \*\* $P$ <0.01; \*\*\* $P$ <0.001 vs normal or for specified comparison by ANOVA with *post hoc* analysis.

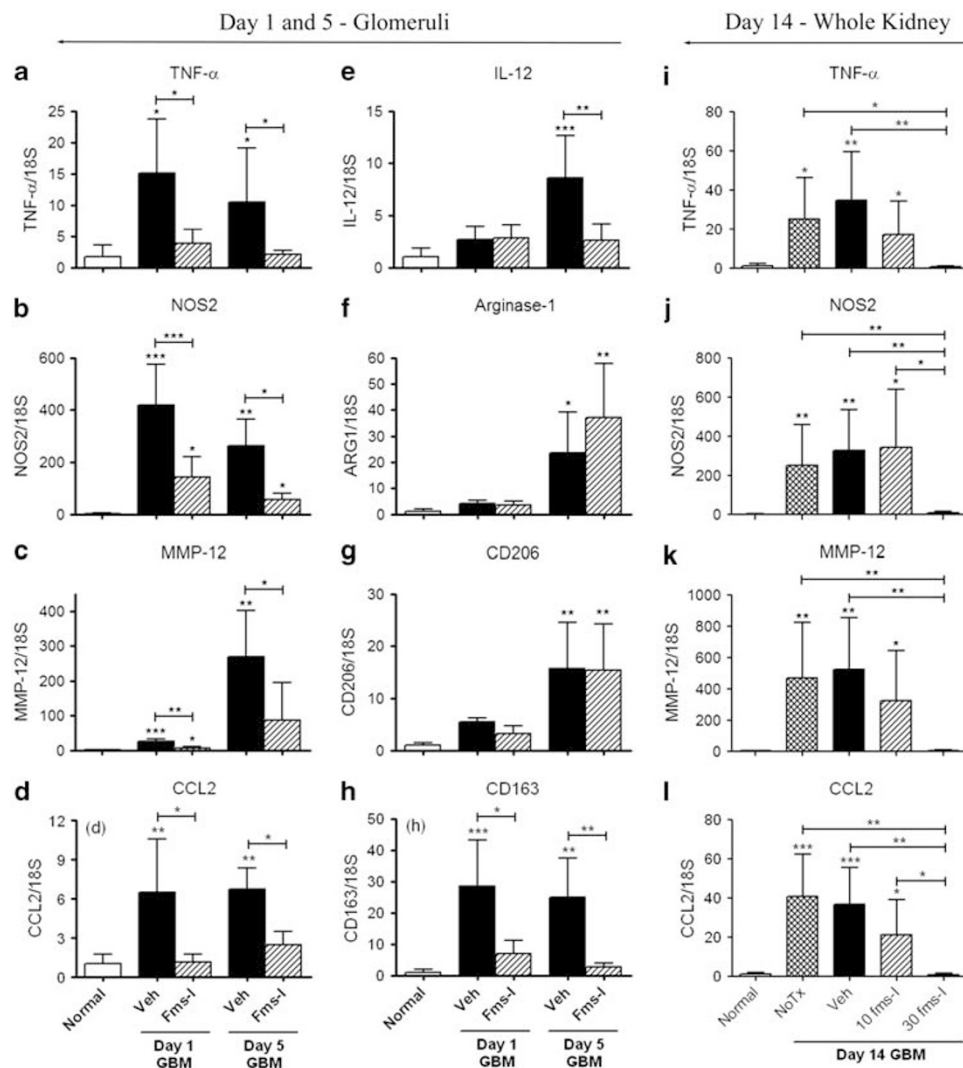


**Figure 9** Analysis of mRNA levels by real-time RT-PCR. Analysis of isolated glomeruli from days 1 and 5 of anti-GBM disease for **(a)** TNF- $\alpha$ ; **(b)** NOS2; **(c)** MMP-12; **(d)** CCL2; **(e)** IL-12; **(f)** arginase-1; **(g)** CD206; **(h)** CD163. Analysis of whole kidney tissue on day 14 of anti-GBM disease for **(i)** TNF- $\alpha$ ; **(j)** NOS2; **(k)** MMP-12; **(l)** CCL2. A group of normal rats (no disease) is also shown. Data are mean  $\pm$  s.d. \* $P$ <0.05; \*\* $P$ <0.01; \*\*\* $P$ <0.001 vs normal or for specified comparison by ANOVA with *post hoc* analysis.

These studies indicate that targeting c-fms kinase activity has therapeutic potential based upon the profound inhibition of renal damage and renal dysfunction seen with fms-I

treatment in the anti-GBM disease model. fms-I had a selective effect upon monocyte/macrophages without depleting blood neutrophils—an important point for host

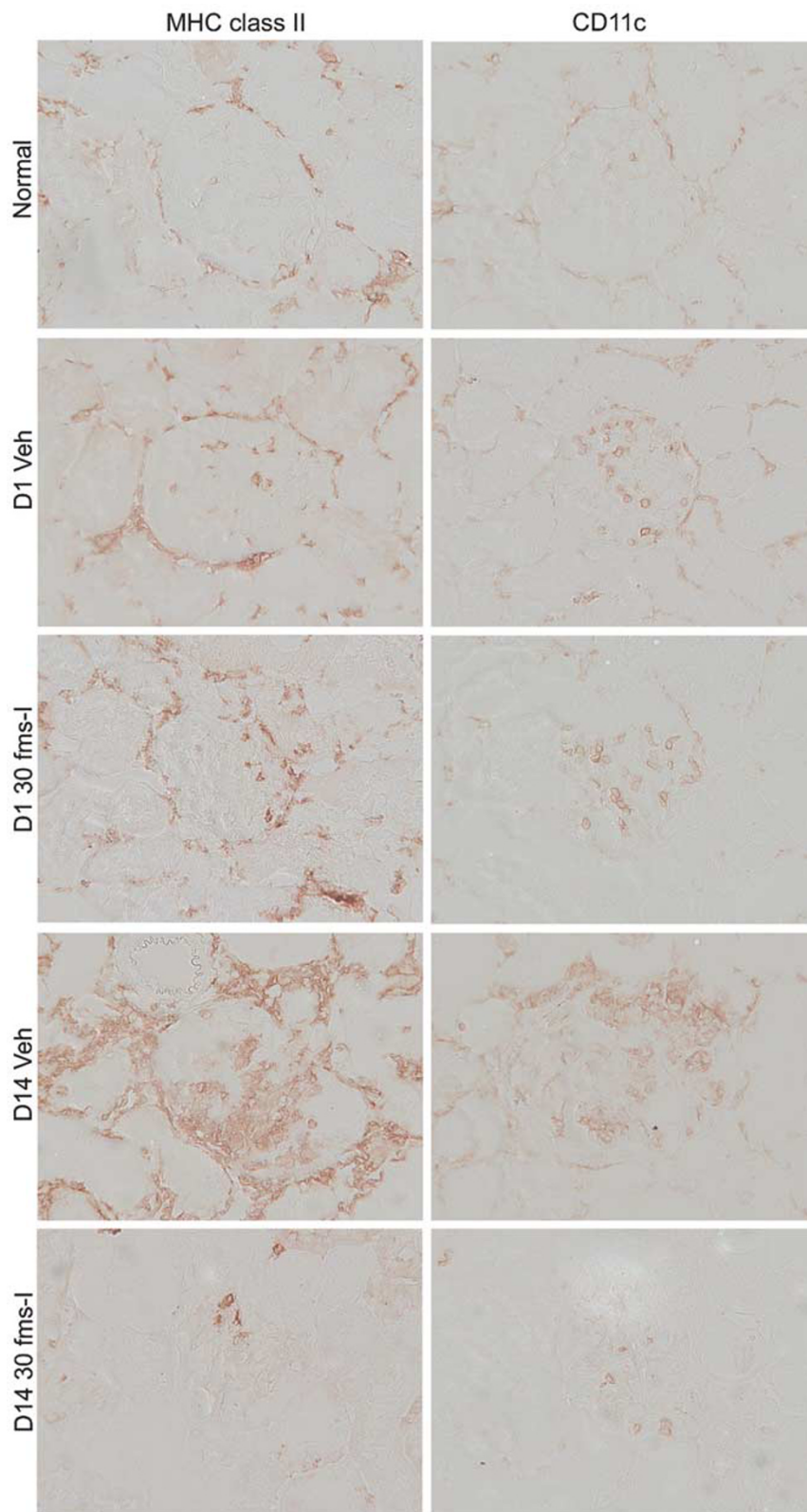


**Figure 10** Immunostaining for dendritic cell markers MHC class II (left panel) and CD11c (right panel) is shown in normal rat kidney, day 1 and day 14 anti-GBM disease with vehicle treatment (Veh), and day 1 and 14 anti-GBM disease with high-dose fms-I treatment (30 mg/kg fms-I). Magnification,  $\times 400$ .

defense—and a minor effect on lymphocyte numbers was only seen with high-dose fms-I. The reduction in blood monocyte and lymphocyte counts is consistent with that previously described in the c-fms gene knockout mouse,<sup>18</sup> and fms-I was well tolerated with animals showing no adverse effects. Furthermore, low-dose fms-I exhibited a significant protective effect on renal damage and dysfunction without affecting blood monocyte counts.

fms-I treatment failed to prevent the induction and maintenance of heavy proteinuria. The small dose of anti-GBM serum used in the WKY rat model does not induce significant heterologous injury in the first 24 h, but proteinuria develops rapidly thereafter. Proteinuria in rat models of anti-GBM disease is macrophage dependent,<sup>4,5,19</sup> and the early glomerular macrophage infiltrate seen in the high-dose fms-I-treated group was likely sufficient to induce proteinuria. Indeed, there was a reduction in podocyte numbers on day 1 of disease preceding the development of proteinuria. However, reversal of the macrophage infiltrate did not reverse proteinuria which was a somewhat surprising result. This may be due to two different possible explanations. First, it may reflect an inability to replace lost podocytes or to recover from podocyte damage in this short timeframe. Second, it may be that proteinuria was partially alleviated by fms-I treatment but that this effect was masked by the substantially higher glomerular filtration rate seen in these animals compared with vehicle and no treatment groups.

Podocyte damage is a precursor to the development of glomerulosclerosis.<sup>20</sup> In fms-I-treated anti-GBM disease, podocyte damage was already evident on day 1 and further podocyte loss was seen on day 14. However, reversing the macrophage infiltrate prevented significant glomerulosclerosis despite podocyte damage in terms of podocyte loss and heavy proteinuria and glomerular tuft adhesions. While it is possible to argue that the protection from glomerulosclerosis with fms-I treatment is due to the partial reduction in podocyte loss, it appears more likely that the main reason for protection is due to suppression of the pro-inflammatory macrophage infiltrate. Similarly, podocyte bridges between the glomerular tuft and Bowman's capsule are considered a critical early event in crescent formation in anti-GBM disease.<sup>21,22</sup> However, glomerular tuft adhesions to Bowman's capsule did not result in crescent formation in high-dose fms-I-treated rats. It has been argued that early cellular crescents in experimental anti-GBM disease are largely composed of proliferating epithelial cells and that macrophages only appear later in the process.<sup>21,22</sup> However, this study clearly demonstrates that macrophages have a critical role in early crescent formation, fibrin deposition in Bowman's space and progression to a fibrocellular phase with Bowman's capsule rupture. This finding is consistent with a study of anti-GBM disease in transgenic mice in which removal of renal macrophages via diphtheria toxin-induced apoptosis significantly reduced crescent formation, glomerular damage and renal dysfunctions.<sup>7</sup>

An M1-type pro-inflammatory phenotype of the infiltrating macrophages is required for macrophage-mediated renal injury in anti-GBM disease.<sup>13,23,24</sup> Real-time RT-PCR analysis of glomeruli on days 1 and 5 of anti-GBM disease indicated a pro-inflammatory, M1-like phenotype of the macrophage infiltrate, although expression of some M2-type markers of alternative macrophage activation was also evident. The progressive reduction in glomerular macrophages seen with high-dose fms-I treatment caused a profound reduction in expression of M1-type pro-inflammatory markers and a relative increase in the expression of some M2-type markers. Thus, while the reduction in the number of macrophages with an M1-like phenotype is likely to be a major mechanism by which fms-I treatment protected against disease progression, an augmentation of alternative activation of the remaining macrophages may have also contributed to this protective effect.

It is argued that proteinuria is an important factor in progressive tubulointerstitial damage. One way in which this may operate is by high levels of albumin in the glomerular filtrate inducing activation of tubular epithelial cells to produce chemokines, such as CCL2 (MCP-1) and osteopontin, that recruit interstitial macrophages which cause progressive tubular damage.<sup>25</sup> However, the upregulation of tubular chemokine expression could also be due to glomerular production of pro-inflammatory cytokines.<sup>26</sup> Indeed, it is difficult to separate these two possible mechanisms *in vivo*. However, in this study we found that high-dose fms-I treatment prevented upregulation of CCL2 and osteopontin expression despite the presence of proteinuria, suggesting that glomerular inflammation may be the dominant mechanism for this tubular response—at least within the short timeframe of these studies.

The role of dendritic cells in immunologic kidney disease has seen renewed interest.<sup>15,27–29</sup> An important issue concerns the source of dendritic cells present at sites of inflammation;<sup>30,31</sup> are they derived from a distinct myeloid precursor population, migratory 'conventional' dendritic cells or derived from monocytes? It is well established that blood monocytes can be differentiated into dendritic cells *in vitro*, but whether this is a major mechanism for dendritic cell production *in vivo* is controversial,<sup>30,31</sup> particularly as the development of most dendritic cell populations is independent of M-CSF signaling.<sup>32,33</sup> The identification of dendritic cells is a difficult matter as they share expression of many antigens with macrophages.<sup>28,34</sup> MHC class II antigens are strongly expressed by all dendritic cells, but they can also be expressed by macrophages and other cell types. In contrast, CD11c is a relatively specific dendritic cell marker.<sup>28,34</sup> Our study suggests that the renal dendritic cells seen on day 14 of anti-GBM disease, as identified by expression of MHC class II and CD11c, are dependent upon M-CSF/c-fms signaling and thus are most probably monocyte derived. This argument is supported by the presence of infiltrating glomerular CD11c+ cells on day 1 of disease. The finding that

interstitial MHC class II+ and CD11c+ cells with a dendritic morphology were largely removed on day 14 of disease by fms-I treatment suggests that M-CSF/c-fms signaling is required for recruitment of these cells (presumably as blood monocytes which were depleted by high-dose fms-I) and for their survival/maintenance within the kidney. However, we cannot exclude the possibility that the dendritic cell population seen in anti-GBM disease derives through local differentiation of a separate blood leukocyte lineage and that the accumulation of these cells is diminished when renal injury is suppressed. These interesting observations may prompt further investigation of the role of M-CSF/c-fms signaling in dendritic cell recruitment and function in inflamed tissues.

The protective effects of fms-I treatment in rat anti-GBM disease appear to be independent of the adaptive immune response. Low-dose fms-I provided significant protection without affecting blood lymphocyte counts, or the biphasic pattern of glomerular T-cell infiltration on days 1 and 14. High-dose fms-I caused a modest reduction in blood lymphocyte counts by day 14 of anti-GBM disease, but did not affect the early glomerular T-cell infiltrate on day 1. The reduction in glomerular T cells seen on day 14 with high-dose fms-I may simply relate to reduced glomerular damage resulting in diminished production of T-cell chemokines. Neither dose of fms-I treatment affected glomerular deposition of rat IgG or C3 indicating no effect upon the humoral immune response.

In conclusion, this study has shown that blockade of c-fms kinase can reverse glomerular macrophage infiltration in rat anti-GBM disease revealing a critical role for macrophages in crescent formation and tubular cell activation independent of podocyte damage and proteinuria, respectively. Finally, this study has identified c-fms kinase inhibition as a potential therapeutic strategy in rapidly progressive crescentic glomerulonephritis.

#### ACKNOWLEDGEMENT

This study was funded by the National Health and Medical Research Council of Australia.

#### DISCLOSURE/CONFLICT OF INTEREST

CLM is an employee of Johnson and Johnson. DJN-P has acted as a consultant for Johnson and Johnson.

- Kerr PG, Nikolic-Paterson DJ, Atkins RC. Rapidly progressive glomerulonephritis. In: Schrier RW (ed). *Diseases of the Kidney and Urinary Tract*, 8th edn. Lippincott Williams and Wilkins: Boston, 2007, pp 1511–1535.
- Little MA, Pusey CD. Glomerulonephritis due to antineutrophil cytoplasm antibody-associated vasculitis: an update on approaches to management. *Nephrology (Carlton)* 2005;10:368–376.
- Holdsworth SR, Neale TJ, Wilson CB. Abrogation of macrophage-dependent injury in experimental glomerulonephritis in the rabbit. Use of an antimacrophage serum. *J Clin Invest* 1981;68:686–698.
- Ikezumi Y, Hurst LA, Masaki T, *et al*. Adoptive transfer studies demonstrate that macrophages can induce proteinuria and mesangial cell proliferation. *Kidney Int* 2003;63:83–95.
- Isome M, Fujinaka H, Adhikary LP, *et al*. Important role for macrophages in induction of crescentic anti-GBM glomerulonephritis in WKY rats. *Nephrol Dial Transplant* 2004;19:2997–3004.
- Lenda DM, Stanley ER, Kelley VR. Negative role of colony-stimulating factor-1 in macrophage, T cell, and B cell mediated autoimmune disease in MRL-Fas(lpr) mice. *J Immunol* 2004;173:4744–4754.
- Duffield JS, Tipping PG, Kipari T, *et al*. Conditional ablation of macrophages halts progression of crescentic glomerulonephritis. *Am J Pathol* 2005;167:1207–1219.
- Pixley FJ, Stanley ER. CSF-1 regulation of the wandering macrophage: complexity in action. *Trends Cell Biol* 2004;14:628–638.
- Isbel NM, Nikolic-Paterson DJ, Hill PA, *et al*. Local macrophage proliferation correlates with increased renal M-CSF expression in human glomerulonephritis. *Nephrol Dial Transplant* 2001;16:1638–1647.
- Isbel NM, Hill PA, Foti R, *et al*. Tubules are the major site of M-CSF production in experimental kidney disease: correlation with local macrophage proliferation. *Kidney Int* 2001;60:614–625.
- Menke J, Rabacal WA, Byrne KT, *et al*. Circulating CSF-1 promotes monocyte and macrophage phenotypes that enhance lupus nephritis. *J Am Soc Nephrol* 2009;20:2581–2592.
- Ma FY, Liu J, Kitching AR, *et al*. Targeting renal macrophage accumulation via c-fms kinase reduces tubular apoptosis but fails to modify progressive fibrosis in the obstructed rat kidney. *Am J Physiol Renal Physiol* 2009;296:F177–F185.
- Ma FY, Flanc RS, Tesch GH, *et al*. Blockade of the c-Jun amino terminal kinase prevents crescent formation and halts established anti-GBM glomerulonephritis in the rat. *Lab Invest* 2009;89:470–484.
- Lan HY, Nikolic-Paterson DJ, Mu W, *et al*. Local macrophage proliferation in the progression of glomerular and tubulointerstitial injury in rat anti-GBM glomerulonephritis. *Kidney Int* 1995;48:753–760.
- Heymann F, Meyer-Schwesinger C, Hamilton-Williams EE, *et al*. Kidney dendritic cell activation is required for progression of renal disease in a mouse model of glomerular injury. *J Clin Invest* 2009;119:1286–1297.
- Wang JM, Griffin JD, Rambaldi A, *et al*. Induction of monocyte migration by recombinant macrophage colony-stimulating factor. *J Immunol* 1988;141:575–579.
- Kluth DC, Ainslie CV, Pearce WP, *et al*. Macrophages transfected with adenovirus to express IL-4 reduce inflammation in experimental glomerulonephritis. *J Immunol* 2001;166:4728–4736.
- Dai XM, Ryan GR, Hapel AJ, *et al*. Targeted disruption of the mouse colony-stimulating factor 1 receptor gene results in osteopetrosis, mononuclear phagocyte deficiency, increased primitive progenitor cell frequencies, and reproductive defects. *Blood* 2002;99:111–120.
- Behmoaras J, Bhargal G, Smith J, *et al*. Jund is a determinant of macrophage activation and is associated with glomerulonephritis susceptibility. *Nat Genet* 2008;40:553–559.
- D'Agati VD. Podocyte injury in focal segmental glomerulosclerosis: lessons from animal models (a play in five acts). *Kidney Int* 2008;73:399–406.
- Le Hir M, Keller C, Eschmann V, *et al*. Podocyte bridges between the tuft and Bowman's capsule: an early event in experimental crescentic glomerulonephritis. *J Am Soc Nephrol* 2001;12:2060–2071.
- Moeller MJ, Soofi A, Hartmann I, *et al*. Podocytes populate cellular crescents in a murine model of inflammatory glomerulonephritis. *J Am Soc Nephrol* 2004;15:61–67.
- Ikezumi Y, Atkins RC, Nikolic-Paterson DJ. Interferon-gamma augments acute macrophage-mediated renal injury via a glucocorticoid-sensitive mechanism. *J Am Soc Nephrol* 2003;14:888–898.
- Ikezumi Y, Hurst L, Atkins RC, *et al*. Macrophage-mediated renal injury is dependent on signaling via the JNK pathway. *J Am Soc Nephrol* 2004;15:1775–1784.
- Zoja C, Garcia PB, Remuzzi G. The role of chemokines in progressive renal disease. *Front Biosci* 2009;14:1815–1822.
- Yu XQ, Fan JM, Nikolic-Paterson DJ, *et al*. IL-1 up-regulates osteopontin expression in experimental crescentic glomerulonephritis in the rat. *Am J Pathol* 1999;154:833–841.
- Scholz J, Lukacs-Kornek V, Engel DR, *et al*. Renal dendritic cells stimulate IL-10 production and attenuate nephrotoxic nephritis. *J Am Soc Nephrol* 2008;19:527–537.
- Rogers NM, Matthews TJ, Kausman JY, *et al*. Review article: kidney dendritic cells: their role in homeostasis, inflammation and transplantation. *Nephrology (Carlton)* 2009;14:625–635.

29. Sung SS, Bolton WK. T cells and dendritic cells in glomerular disease: the new glomerulotubular feedback loop. *Kidney Int* 2010;77:393–399.
30. Leon B, Ardavin C. Monocyte-derived dendritic cells in innate and adaptive immunity. *Immunol Cell Biol* 2008;86:320–324.
31. Segura E, Villadangos JA. Antigen presentation by dendritic cells *in vivo*. *Curr Opin Immunol* 2009;21:105–110.
32. Witmer-Pack MD, Hughes DA, Schuler G, *et al*. Identification of macrophages and dendritic cells in the osteopetrotic (op/op) mouse. *J Cell Sci* 1993;104(Part 4):1021–1029.
33. Liu K, Victora GD, Schwickert TA, *et al*. *In vivo* analysis of dendritic cell development and homeostasis. *Science* 2009;324:392–397.
34. Ferenbach D, Hughes J. Macrophages and dendritic cells: what is the difference? *Kidney Int* 2008;74:5–7.